Comput Geosci (2006) 10: 279–290
DOI 10.1007/s10596-006-9023-9

Semi-analytical solutions of a contaminant transport equation with nonlinear sorption in 1D

Peter Frolkovič · Jozef Kačur

Received: 4 October 2004 / Revised: 15 February 2005 / Accepted: 16 December 2005 / Published online: 4 July 2006

Abstract A new method to determine semi-analytical solutions of one-dimensional contaminant transport problem with nonlinear sorption is described. This method is based on operator splitting approach where the convective transport is solved exactly and the diffusive transport by finite volume method. The exact solutions for all sorption isotherms of Freundlich and Langmuir type are presented for the case of piecewise constant initial profile and zero diffusion. Very precise numerical results for transport with small diffusion can be obtained even for larger time steps (e.g., when the Courant-Friedrichs-Lewy (CFL) condition failed).

Keywords contaminant transport · finite volume method · Freundlich isotherm · nonlinear sorption

AMS Subject Classification 35K65 · 35L67 · 65M25

Peter Frolkovič (✉)
Simulation in Technology Center,
University of Heidelberg,
Im Neuenheimer Feld 368,
69120 Heidelberg, Germany
e-mail: peter.frolkovic@uni-hd.de

Jozef Kačur
Department of Mathematical Analysis
and Numerical Mathematics,
Comenius University,
Mlynska dolina,
842 48 Bratislava, Slovakia
e-mail: kacur@fmph.uniba.sk

1. Mathematical model

The main goal of this paper is to construct precise semi-analytical solutions of the nonlinear convection–diffusion problem with adsorption

$$\partial_t F(u) + v(x)\partial_x u - \partial_x(D(x)\partial_x u) = 0 \tag{1}$$

for $x \in (0, L),\ t > 0$, with initial condition

$$u(x, 0) = U^\circ(x) \tag{2}$$

and boundary conditions

$$u(0, t) = C^\circ(t), \qquad \partial_x u(L, t) = 0\,. \tag{3}$$

Here,

$$D(x) \geq D_0 > 0, \quad v(x) \geq v_0 > 0, \quad F(0) = 0, \quad F'(s) \geq \delta,$$

where one can assume that $\delta = 1$.

The mathematical models (1)–(3) can represent contaminant transport in equilibrium mode with the sorption isotherm $\Psi(u) = F(u) - u$ (see, e.g., [9]). The corresponding mathematical model is

$$\partial_t u + v(x)\partial_x u - \partial_x(D(x)\partial_x u) + \partial_t S = 0,$$

$$\partial_t S = k(\Psi(u) - S),$$

where $S = \Psi(u)$ for $k \to \infty$. Most common forms of (nonlinear) sorption isotherms are Freundlich

$$\Psi(u) = au^p, \quad a, p > 0 \tag{4}$$

and Langmuir

$$\Psi(u) = \frac{au}{1 + bu}, \quad a, b > 0\,, \tag{5}$$

but one can also consider isotherms of mixed type

$$\Psi(u) = \frac{au^p}{1 + bu^p}\,. \tag{6}$$

Equation (1) can be written in the form,

$$F'(u)\,\partial_t u + v(x)\partial_x u - \partial_x(D(x)\partial_x u) = 0\,, \qquad (7)$$

where the function $F'(u) \geq 1$ can be viewed as a (nonlinear) "retardation" factor of the convective and diffusive transport.

In the case of $F'(0) = \infty$ [i.e., for (4) and (6) with $0 < p < 1$], the solution of (1) can have a sharp front with a finite speed of propagation [27]. Moreover, the convective term can be dominant and thus the creation of shocks can be expected even for smooth initial data. Nevertheless, because of the presence of (small) diffusion $D_0 > 0$, the solution of (1)–(3) is regular and sharp shocks (as known for hyperbolic problems) can not develop in a finite time – see, e.g., [15].

Precise numerical solutions of (1) are required, for instance, if one wishes to solve inverse problems (e.g., to determine the diffusion D and the sorption isotherm) or to test numerical methods for this type of problems. Most numerical methods so far are based on regularisation and/or upwinding procedures and they can produce undesirable artefacts in numerical solutions. The main goal of this paper is to avoid any regularisation of $F(u)$ and to significantly decrease numerical dispersion. Consequently, precise numerical solutions of (1)–(3) can be obtained even for the case of vanishing diffusion and for very large retardation factor $F'(u)$.

Characteristics-based numerical discretisations of contaminant transport with nonlinear adsorption were described in [3, 4, 8, 15], and upwind-based discretization methods for the same type of problems in [6, 22]. Asymptotic formulas for large-time behaviour of the exact solution of (1) were obtained in [7, 10], but they can not be used directly in discretization methods.

The method presented in this paper is based on operator splitting, where nonlinear transport and nonlinear diffusion are solved separately along each time step – see, e.g., [12]. The transport part is solved exactly for piecewise constant initial profile and the diffusion part by some standard finite volume method. Consequently, our method has very weak restriction on time steps, and the Courant number can be larger than 1. In fact, if smaller diffusion is considered (i.e., the Peclet number is larger), than larger time steps can be taken in numerical simulations.

Analytical solutions for the purely convective case of contaminant transport with nonlinear sorption using simple initial and boundary data have been described by Sheng and Smith [26]. Independently, a general case of piecewise constant initial and boundary data was solved by different analytical methods in [16] for the same equation, where long-time behaviours such as collapses of shocks were likewise considered. Our paper summarises and extends the results presented by Kačur and Frolkovič [16].

The paper is organised as follows. In section 2, we describe the method of solution for (1)–(3) using an operator splitting approach. In section 3 we deal in details with purely convective transport and present analytical formulas for solution of multiple Riemann problems with Freundlich and Langmuir isotherms. In section 4 the method for solving of nonlinear diffusive transport is discussed.

Finally, section 5 presents some numerical results and concluding discussions. The routines in Maple language [20] that were used for the exact solutions of nonlinear convection transport and the programme in C language for numerical solving of nonlinear convection–diffusion transport with Freundlich isotherms (using software library Numerical Recipes [25]) are available by request from the first author.

2. Operator splitting method

Let $\tau := t_j - t_{j-1}$ be a time step and $u_{j-1} \approx u(x, t_{j-1})$ be an approximation of the solution $u(x,t)$ at the time level t_{j-1}. The method, considered here, determines numerical solution u_j in a two-step procedure

$$u_j = D^j(\tau)T^j(\tau)u_{j-1},$$

where $T^j(\tau)$ represents the solution of the convection part of (1) and $D^j(\tau)$ represents the solution of the diffusion part of (1).

More precisely, we start with solving the hyperbolic problem

$$\partial_t F(\phi) + v(x)\partial_x \phi = 0, \qquad t \in (t_{j-1}, t_j), \qquad (8)$$

with the inflow boundary condition $\phi(0,t) = C^\circ(t)$ and the initial condition $\phi(x, t_{j-1}) = u_{j-1}$. This first step defines

$$u_j^{1/2} := T^j(\tau)u_{j-1} \equiv \phi(x, t_j)\,, \qquad (9)$$

and then we solve the problem

$$\partial_t F(\phi) - \partial_x(D(x)\partial_x \phi) = 0, \qquad t \in (t_{j-1}, t_j), \qquad (10)$$

with the boundary conditions

$$\phi(0,t) = C^\circ(t), \qquad \partial_x \phi(L,t) = 0,$$

and the initial condition $\phi(x, t_{j-1}) = u_j^{1/2}$. This second step defines

$$u_j := D^j(\tau)u_j^{1/2} \equiv \phi(x, t_j).$$

In our practical realisation, the transport step $T^j(\tau)$ is solved exactly for initial piecewise constant data and for boundary conditions of the form

$$C^\circ(t) \equiv C_j^\circ\,,\ \ t \in (t_{j-1}, t_j), \tag{11}$$

and the diffusion step $D^j(\tau)$ is approximated using a finite volume method (FVM). In the case of a non-constant velocity $v(x)$, a transformation to a new space variable y is used in both steps.

In general, the result of the transport step is not a piecewise constant function with respect to the fixed grid that shall be used in the diffusion step, and one has to project $u_j^{1/2}$ to this grid. From the point of view of mass conservation, it is important that this projection is precise. In fact, we compute such projection exactly for a general type of isotherms $\Psi(u)$.

The output u_j of the diffusion step (realised by FVM) is again piecewise constant, so the next transport step along $t \in (t_j, t_{j+1})$ can be realised. Thus, the projection represents the only source of numerical dispersion that can be controlled by a smaller space discretization and relatively large time steps.

In general, the operator splitting method, as given here, can be further improved in a straightforward way to reduce time splitting error, see, e.g., descriptions and references in [19] for Strang splitting.

3. Solution of the transport problem

Firstly, to solve (8), we use the transformation

$$y = G(x) = \int_0^x \frac{dz}{v(z)} \tag{12}$$

and rewrite (8) into a simpler form

$$\partial_t F(u) + \partial_y u = 0, \qquad t \in (t_{j-1}, t_j)\,, \tag{13}$$

where $u(y,t) = u(G(x),t) := \phi(t,x)$. The initial condition are given by $u(G(x),0) = U^\circ(x)$ and the boundary condition by $u(0,t) = C^\circ(t)$.

The solution of (13) presented in this paper is based on theoretical results in [5, 17, 18, 23, 24], etc., which guarantee the existence, uniqueness and some properties of entropy solutions for hyperbolic problems.

The theoretical treatment of entropy solution has been developed for hyperbolic equations in the form

$$\partial_t w + \partial_y f(w) = 0, \quad w(y,0) = W^\circ(y) = F(U^\circ(x)) \tag{14}$$

that can be obtained from (13) by the transformation $F(u) = w$, i.e., $u = f(w)$, where $f = F^{-1}$ is an inverse function of F. Unfortunately, in general, the function f can not be determined in an analytical form. In this section, we construct analytical solutions of (13) without having an explicit form of the function f.

Our construction of the entropy solution is based on analytical solutions of a multiple Riemann problem [5, 12, 19], and it substantially depends on the structural properties of F. In particular, if F is concave (or convex) and the inverse function of $1/F'(\cdot)$ can be expressed in an analytical form, we can construct the solution of (13) in an analytical form, too.

In the following remark, we list some properties of the solution of multiple Riemann problem which are sufficient for the construction of solution for (14) in an analytical form.

Remark 1. *If F is concave (i.e., f is convex), then a jump in $W^\circ(y)$ at $y = y^*$ is called an* acceptable shock, *if*

$$W^\circ(y_-^*) := \lim_{y \nearrow y^*} W^\circ(y) > W^\circ(y_+^*) := \lim_{y \searrow y^*} W^\circ(y).$$

In that case, the shock at $y = y^*$ will move in time in y-direction with the Rankine–Hugoniot speed v,

$$v = \frac{f(W^\circ(y_-^*)) - f(W^\circ(y_+^*))}{W^\circ(y_-^*) - W^\circ(y_+^*)}\,.$$

If $W^\circ(y_-^*) < W^\circ(y_+^*)$, then a jump at $y = y*$ is called not acceptable shock *and is replaced in time by a* rarefaction wave w^*, *which is a smooth function of the form*

$$w^*\left(y - y^*, t\right) = (f')^{-1}\left(\frac{y - y^*}{t}\right), \tag{15}$$

that is defined for $t > 0$ and

$$y^* + f'(W^\circ(y_-^*))\,t < y < y^* + f'(W^\circ(y_+^*))\,t\,.$$

This construction is valid until no "collision" between shocks and rarefaction waves appears.

To construct the rarefaction wave function w^* in (15), one needs to find the inverse function of $f'(\cdot)$. If the inverse function of $\Psi'(\cdot)$ is known in an analytical form, this can be realised as we describe now.

Denoting $v := f'(w)$ and using

$$v = f'(w) = \frac{1}{F'(u)} = \frac{1}{1 + \Psi'(u)}\,, \tag{16}$$

one obtains

$$u = \left(\Psi'\right)^{-1}\left(\frac{1 - v}{v}\right). \tag{17}$$

Using (16), (17) and $w = F(u)$, one finally gets

$$(f')^{-1}(v) = w = F\left(\left(\Psi'\right)^{-1}\left(\frac{1 - v}{v}\right)\right). \tag{18}$$

If an analytical form of $(\Psi')^{-1}$ is not known, one can compute (17) for some particular values of v numerically.

If f is concave (i.e., when F is convex), then the role of acceptable and not acceptable shocks is exchanged. In particular, if $W^\circ(y_-^*) > W^\circ(y_+^*)$, then the shock is not acceptable and it develops into the rarefaction wave w^*. Again, the function w^* is generated by (15), but it has a different shape now.

Summarising, the solution w of (14) for a piecewise constant initial function W° consists (for some time) of constants and rarefaction waves w^* generated by (15). Next, we describe the construction of w in details.

3.1. Analytical solution of multiple Riemann problem

Firstly, we simplify the treatment of boundary conditions by considering only the case $C^\circ(t) \equiv W^{(0)} \geq 0$ in (3). Our description can be extended for the case when $C^\circ(t)$ is a piecewise constant function in time, like in (11), but we skip details here.

Let the initial function W° have a piecewise constant profile, i.e.,

$$W^\circ(y) = \begin{cases} W^{(i)}, \text{ for } y_{i-1} < y \leq y_i, & i = 1, ..., M, \\ W^{(0)}, \text{ for } y \leq y_0. \end{cases} \tag{19}$$

If $W_i \neq W_{i+1}$, the point y_i is a shock. To distinguish between acceptable and not acceptable shocks, we use the notation $y_i^{(a)}$, resp. $y_i^{(na)}$. The development of shocks in time will be described by $y_i(t) = y_i + v_i t$, where

$$v_i = \begin{cases} f'\left(W^{(i)}\right), & \text{if } y_i = y_i^{(na)} \\ \frac{f(W^{(i+1)}) - f(W^{(i)})}{W^{(i+1)} - W^{(i)}}, & \text{if } y_i = y_i^{(a)} \end{cases}.$$

For completeness, we define $v_0 = 0$.

Clearly, for some time interval $(0, t_1)$ there is no collision of two shocks, i.e., $y_{i-1}(t) < y_i(t)$, $i = 1, \ldots, M$, and the solution $w(y, t)$ can be defined for each space interval $(y_{i-1}(t), y_i(t))$ following Remark 1.

In particular, if $y_{i-1} = y_{i-1}^{(a)}$, then

$$w(y, t) = W^{(i)}, \quad y_{i-1}(t) < y < y_i(t), \tag{20}$$

and if $y_{i-1} = y_{i-1}^{(na)}$, then

$$w(y, t) = \begin{cases} w^*(y - y_{i-1}, t) & y_{i-1}(t) < y < y_{i-1} + f'\left(W^{(i)}\right) t, \\ W^{(i)} & y_{i-1} + f'\left(W^{(i)}\right) t < y < y_i(t). \end{cases} \tag{21}$$

To define the time t_1 precisely, we now discuss possible collisions of $y_i(t)$ with $y_{i-1}(t)$. To do so, we first assume that f is convex. Note that in such a case, due to Remark 1, two moving shocks $y_{i-1}(t)$ and $y_i(t)$ can never meet if $y_{i-1} = y_{i-1}^{(na)}$ and $y_i = y_i^{(na)}$.

We must discuss two particular cases. Firstly, if $y_{i-1} = y_{i-1}^{(na)}$ and $y_i = y_i^{(a)}$, then $f'\left(W^{(i)}\right) > v_i$, and the rarefaction wave (from left) will meet the shock (from right) at a time t_i^* (see also figure 7 later). The time t_i^* is given by the equation $y_{i-1}(t_i^*) = y_i(t_i^*)$, i.e.,

$$t_i^* = \frac{y_i - y_{i-1}}{f'\left(W^{(i)}\right) - v_i}.$$

Secondly, if $y_{i-1} = y_{i-1}^{(a)}$ and $y_i = y_i^{(a)}$, then the shocks $y_{i-1}(t)$ and $y_i(t)$ can meet only if $v_{i-1} > v_i$, and, in such a case, it happens at time t_i^{**},

$$t_i^{**} = \frac{y_i - y_{i-1}}{v_{i-1} - v_i}.$$

Summarising, the general solution (20)–(21) is valid for $0 < t < t_1$, where t_1 is the time at which the first collision of shocks appears, i.e.,

$$t_1 = \min_i \{t_i^*, t_i^{**}\}.$$

To extend the description of w for $t > t_1$, we restrict to a special form of initial functions W°.

Definition 1. *We call the function $W^\circ(y)$ in (19) to be* concave *if the values $W^{(i)}$ are non-decreasing for $1 \leq j \leq i_0 < M$ and non-increasing for $i_0 \leq j \leq M$.*

To extend the description (20) and (21) for $t > t_1$, we must discuss two possible cases – collisions of several acceptable shocks and a time development of the shock after collision of acceptable and not acceptable shocks. We still concentrate on case f being a convex function, i.e., one has $y_{i_0-1} = y_{i_0-1}^{(na)}$ and $y_{i_0} = y_{i_0}^{(a)}$, if $W^{(i_0-1)} \neq W^{(i_0)} \neq W^{(i_0+1)}$.

Firstly, if y_{i-1} and y_i are acceptable shocks that met at $t = t_1$, then for $t > t_1$ one has to "remove" the value $W^{(i)}$ and to identify $y_{i-1}(t_1)$ with $y_i(t_1)$, i.e., for $t > t_1$ one has $z(t) := y_{i-1}(t) \equiv y_i(t)$, where the new shock $z(t)$ will move with the velocity

$$v = \frac{f\left(W^{(i+1)}\right) - f\left(W^{(i-1)}\right)}{W^{(i+1)} - W^{(i-1)}}.$$

Following Remark 1, one can now define the analytical solution of (13) for $t \in (0, t_2)$, $t_2 > t_1$, where time t_2 corresponds to the collision of a rarefaction wave from the left (starting from y_{i_0-1}) with the moving acceptable shock $z(t)$.

In fact, $z(t)$ can represent a shock obtained after several collisions in a "decreasing leading front" of $W^\circ(y)$, i.e.,

$$z(t) = y_{i_0}(t) = \ldots = y_{i_0+k-1}(t) \tag{22}$$

with the last "accumulated" velocity

$$v = \frac{f\left(W^{(i_0)}\right) - f\left(W^{(i_0+k)}\right)}{W^{(i_0)} - W^{(i_0+k)}}.$$

In such a case, time t_2 can be determined from the equation for t

$$y_{i_0-1} + f'(W^{(i_0)})t = y_{i_0} + \int_0^t v(s)ds, \tag{23}$$

where $v(s)$ is the shock velocity of y_{i_0} that is changing by jumps after each collision. In general, there is no particular order of the collisions of neighbouring acceptable shocks y_{k-1} and y_k for different k with $k \geq i_0$.

Finally, to construct the solution of (13) for $t > t_2$, one has to describe the movement of the shock at the front of rarefaction wave. The point $s(t_2) = y_{i_0-1} + f'(W^{(i_0)})\, t_2$ represents the acceptable shock at $t = t_2$ that will move further for $t > t_2$ with the Rankine–Hugoniot velocity $\dot{s}(t)$ that is governed by the Ordinary Differential Equation (ODE)

$$\dot{s}(t) = \frac{f\left(w^\star(s(t) - y_{i_0-1}, t)\right) - f\left(W^{(i_0+k)}\right)}{w^\star(s(t) - y_{i_0-1}, t) - W^{(i_0+k)}} \tag{24}$$

and the initial condition

$$s(t_2) = y_{i_0-1} + f'\left(W^{(i_0)}\right) t_2\,. \tag{25}$$

Equation (24) is valid up to the next collision with acceptable shock or up to the moment when $w^\star(s(t) - y_{i_0-1}, t) = W^{(i_0+k)}$, which is a singular point for (24). Nevertheless, in both cases, we are in a situation which was described before.

The case of f being a concave function can be treated analogously.

Next, we describe in detail the application of our construction for the case of Freundlich and Langmuir type of isotherms.

3.2. Freundlich isotherms

In this case, $F(u) = u + au^p$ with $p > 0$. If $p < 1$, then F is concave, and, consequently, f is convex. For $p > 1$, f is concave, so the type of shocks in W° is different. Therefore, we consider each case separately.

3.2.1. *Case* $\mathbf{p} \in (\mathbf{0}, \mathbf{1})$

Generally, one can not express f in an analytical form. Nevertheless, we can construct the rarefaction wave by using (18),

$$w = (f')^{-1}(v) = F\left(\left(\frac{1-v}{pav}\right)^{\frac{1}{p-1}}\right).$$

Following (15), the corresponding rarefaction wave for (14) is of the form

$$w^*(y,t) = F\left(\left(\frac{t-y}{pay}\right)^{\frac{1}{p-1}}\right), \qquad 0 < y < t. \tag{26}$$

Consequently, the corresponding rarefaction wave for (13) is

$$u^*(y,t) = \left(\frac{t-y}{pay}\right)^{\frac{1}{p-1}}, \qquad 0 < y < t. \tag{27}$$

Concerning the evolution of initial profile W°, the solution $w(y,t)$ takes the form (21) for all $y_{i-1} = y_{i-1}^{(na)}$, $i < i_0$, and the form (20) otherwise, i.e., for all $y_i = y_i^{(a)}$, $i \geq i_0$. The pictures in figure 1 illustrate the construction (20) and (21) to determine u using a single rarefaction wave function u^* defined by (27).

This construction is valid until the rarefaction wave does not meet a shock (see section 3.1 for details). The governing equation for the shock propagation after the rarefaction wave meets the acceptable shock $z(t)$ from (22) is governed by the ODE (24) for $t > t_2$, i.e.,

$$\dot{s}(t) = \frac{A(s(t),t) - f\left(W^{(i_0+k)}\right)}{F(A(s(t),t)) - W^{(i_0+k)}},$$

$$s(t_2) = y_{i_0-1} + f'\left(W^{(i_0)}\right) t_2\,, \tag{28}$$

where

$$A(s(t),t) := \left(\frac{t - s(t) + y_{i_0-1}}{pa(s(t) - y_{i_0-1})}\right)^{\frac{1}{p-1}}.$$

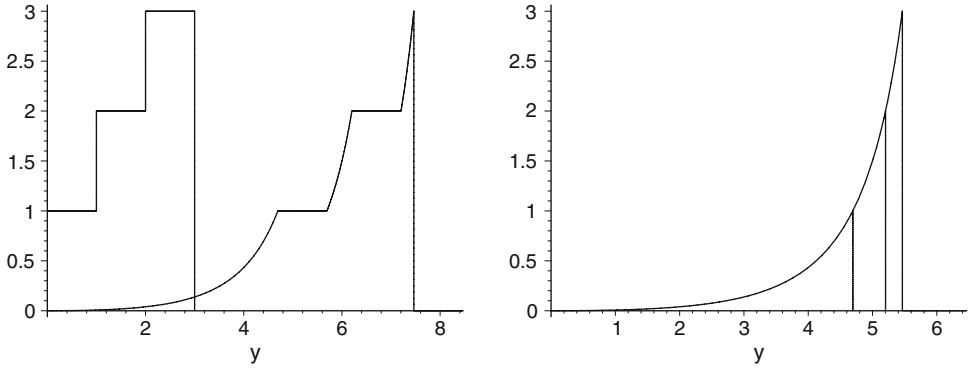

Figure 1 Left: the exact solution of $\partial_t(u + u^{1/2}) + \partial_y u = 0$ for $t = 0$ (i.e., the initial function U°), and for $t = 7.04$. Right: the corresponding rarefaction wave $u^*(y, 7.04)$ defined in (27).

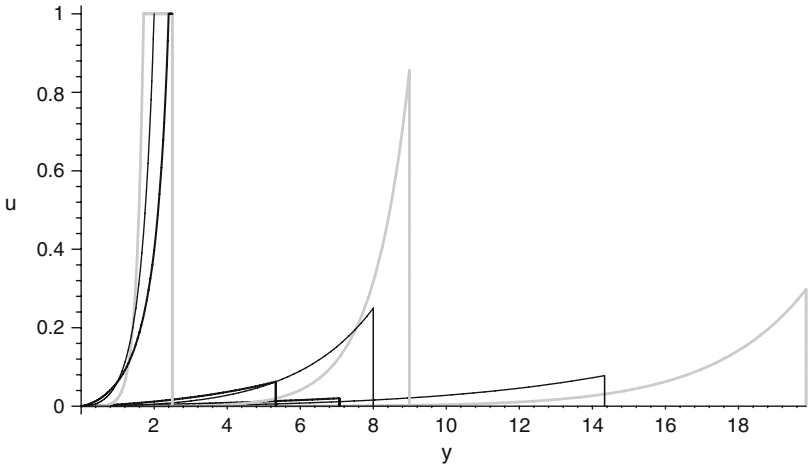

Figure 2 Solutions of $\partial_t(u+u^p)+\partial_y u=0$ for $p=3/4,\ 1/2,\ 1/4$ (from right to left: gray, dash and solid lines) and for three different times $t=3,\ 16,\ 40$.

In general, this ODE must be solved numerically. For some particular values of p, the function $s(t)$ can be obtained by solving a nonlinear algebraic equation (see [16] for some examples).

To characterise the solutions of the transport equation with Freundlich isotherm, we present a representative example of (13). Particularly, we consider the zero inflow concentration $C^\circ(t)\equiv 0$ and the piecewise constant initial impulse $U^\circ(y)=1$ for $y\in(0,1)$ and $U^\circ(y)=0$ otherwise. The following figures were produced using the software Maple [20], and the corresponding Maple routines are available by request from the first author.

Figure 2 shows the time development of solutions of the equation $\partial_t(u+u^p)+\partial_y u=0$ for three different values of parameter $p\in(0,1)$. In each case, the rarefaction wave starts at the point $y=y_0=0$ (in fact, $y_0(t)\equiv 0$), and the tailing part of a rarefaction wave appears behind the acceptable shock that has started initially at $y=1$. For smaller values of p, the rarefaction wave reaches sooner the shock at the front of curves and the decrease in shock value afterwards is faster. Naturally, with smaller values of p the "retardation" of transport (7) is larger, and, consequently, the movement of fronts (or acceptable shocks) is slower.

Figure 3 shows the curves $F(u)$, i.e., the solution w of (14), for the same data. Note that the solutions $w=F(u)$ are "mass conservative".

3.2.2. *Case* $\mathbf{p>1}$

The governing equations are the same as in the case of $p<1$. Particularly, the rarefaction waves $w^*(y,t)$ and $u^*(y,t)$ are given by the same formulas (26) and (27).

Opposite to the previous case, one has $f'\left(W^{(i-1)}\right)\geq f'\left(W^{(i)}\right)$, and acceptable shocks appear on the trailing part of solution curves (i.e., at the points y_i, $i<i_0$), whereas the rarefaction waves appear on the leading front of initial concave profile W° (i.e., at the points y_i, $i\geq i_0$, see Definition 1).

Also, the governing equation for the movement of shock after its collision with the rarefaction wave is given by an analogous ODE to (28), where one has only

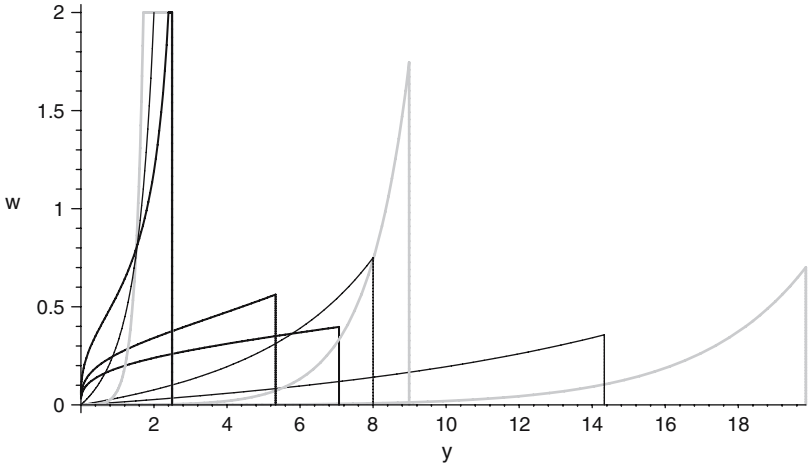

Figure 3 The curves $w=u+u^p$ for solutions of $\partial_t(u+u^p)+\partial_y u=0$ for $p=3/4,\ 1/2,\ 1/4$ (from right to left: gray, dash and solid lines) and for three different times $t=3,\ 16,\ 40$.

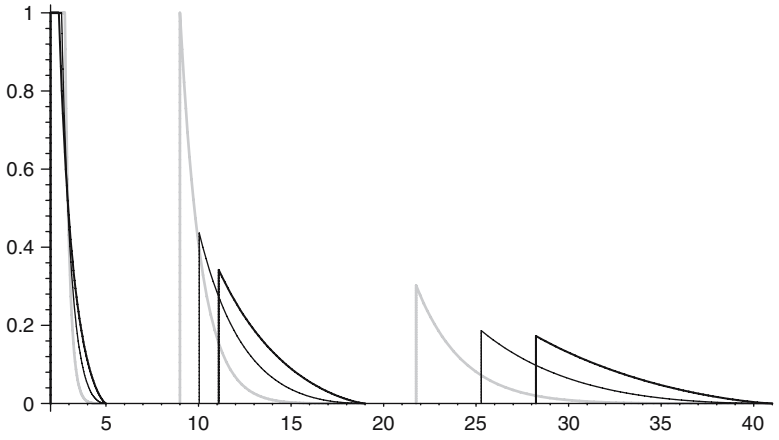

Figure 4 Solutions of $\partial_t(u+u^p)+\partial_y u=0$ for $p=7/4, 3/2, 5/4$ (from left to right: gray, dash and solid line) for three different times $t=4, 18, 40$.

to replace k by $-k$, since the shocks can accumulate on the trailing part of wave.

The solution of equation $\partial_t(u+u^p)+\partial_y u=0$ with the same initial and boundary conditions as in the case $p<1$ are presented in the next figures. Figure 4 shows u for three different values of $p\in(1,2)$ where the (convex) shape of curves is analogous to the case $p\in(0,1)$. Of course, the tailing part of rarefaction waves appears at the front of shocks. For $p\in[2,4]$, the behaviour is analogous, but the shape of curves becomes concave (see figure 5).

3.2.3. *Case* $\mathbf{p=1}$

In this case, all shocks of initial profile are acceptable and the construction of the analytical solution is trivial.

3.3. Langmuir isotherm

In this case, the function $F(s)=as/(1+bs)$ is concave, and, consequently, f is convex. One can express f directly in the analytical form

$$f(w)=\frac{1}{2}\left(w-\frac{a+1}{b}+\frac{1}{b}\sqrt{(bw+1-a)^2+4a}\right),$$

and

$$(f')^{-1}(v)=\frac{1}{b}\left(a-1+2\sqrt{a}\frac{2v-1}{\sqrt{1-(2v-1)^2}}\right).$$

Thus, the rarefaction wave w^* is of the form

$$w^*(y,t)=\frac{1}{b}\left(a-1+2\sqrt{a}\frac{2y-t}{\sqrt{t^2-(2y-t)^2}}\right), \tag{29}$$

and, consequently,

$$u^*(y,t)=\frac{1}{b}\left(-1+\sqrt{a}\frac{2y}{\sqrt{t^2-(2y-t)^2}}\right). \tag{30}$$

The construction of analytical solution for concave initial profile W° is analogous to Case I of Freundlich isotherm with $p<1$. Of course, opposite to the Freundlich case, one has $F'(0)=1+a<\infty$. In particular, the velocity speed of rarefaction wave between $y_0(t)$ up to the shock $y_1(t)$ (provided $C^\circ(t)\equiv 0$) is $f'(0)=(1+a)^{-1}>0$, opposite to the Freundlich case $p<1$, where $y_0(t)\equiv 0$. Consequently, the trailing part of concentration profile is shorter for the Langmuir case.

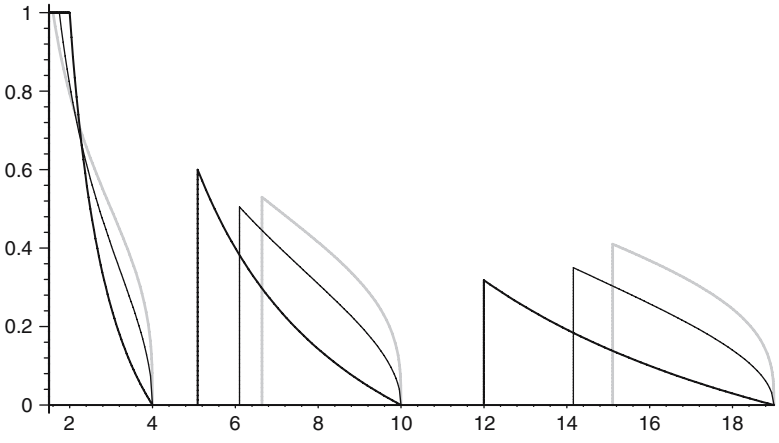

Figure 5 Solutions of $\partial_t(u+u^p)+\partial_y u=0$ for $p=2, 3, 4$ (from left to right: solid, dash and gray line) for three different times $t=3, 9, 18$.

When the rarefaction wave meets the shock in front, i.e., at $t = t_2$, the governing equation for the shock movement is identical to (28), where one has to use $A(s(t), t) := u^*(s(t) - y_{i_0-1}, t)$.

For the initial profile $W^\circ(y)$ of the form $W^\circ(y) \equiv W^\circ$, $y \in (0, L)$, and $W^\circ(y) \equiv 0$ otherwise, one can find an explicit formula for the front movement,

$$s(t) = \frac{1}{2(a+1)^2}\left(14ta + 2Pb(a-1) - 4t\sqrt{a}\sqrt{\left(1+\frac{Pb}{t}\right)\left(a-\frac{Pb}{t}\right)}\right)$$

for

$$t > t_1 = \frac{P}{f'(W^\circ)W^\circ - f(W^\circ)},$$

where $P = W^\circ L$.

The solutions of equation $\partial_t(u + au/(1+u)) + \partial_y u = 0$ for three different values of a, with the identical boundary and initial conditions as before, are presented in figure 6.

3.4. General concave and convex isotherms Ψ

For a general case of an isotherm Ψ that is either convex or concave, the inverse function of Ψ' needs not be known in an analytical form. Nevertheless, one can numerically construct the rarefaction wave for some finite set of points by solving a nonlinear algebraic equation.

In particular, to obtain $u^*(y - y^*, t)$, one can follow the approach in (17) and solve the following nonlinear scalar algebraic equation

$$\Psi'\left(u^*\left(y - y^*, t\right)\right) = \frac{t - y + y^*}{y - y^*}.$$

with respect to u^* by means of, for instance, an iterative Newton method.

In the case when an isotherm is neither convex nor concave, one can numerically compute the rarefaction waves following Osher's solution (see, e.g., [19] for details).

4. Solution of the nonlinear diffusion problem

In the previous section, we derived analytical formulas for the solution of nonlinear convection equation (13) with piecewise constant initial function that was defined on some grid $0 = y_0 < y_1 < \ldots < y_M = G(L)$. It is more convenient to transform the nonlinear diffusion equation (10) to y, too. It means that in the second step of the operator splitting method, we have to solve the equation

$$\partial_t F(u) - a(y)\partial_y(b(y,t)\partial_y u) = 0, \tag{31}$$

with the boundary condition

$$u(0,t) = C^\circ(t), \quad \partial_y u(G(L), t) = 0, \tag{32}$$

and the initial condition

$$u(y, t_{j-1}) = u_j^{1/2}(y), \tag{33}$$

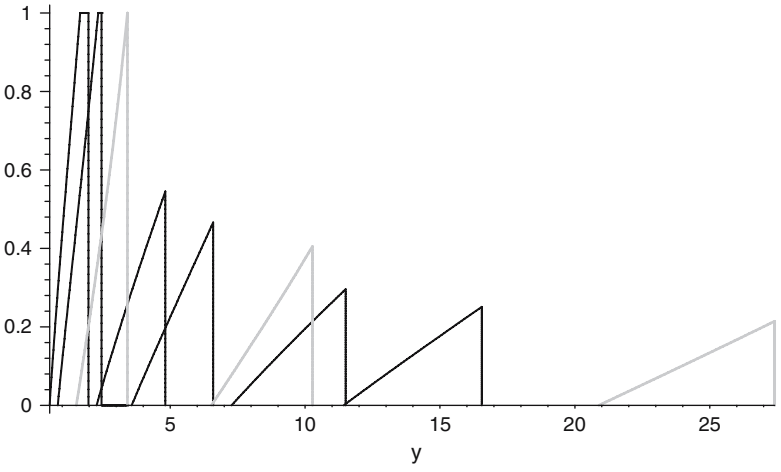

Figure 6 Solutions of $\partial_t(u + au/(1+u)) + \partial_y u = 0$ for $a = 2.83, 6, 10$ (from left to right: solid, dash and gray line) and for three different times $t = 5.83, 25, 80$.

where the coefficients a and b are given by

$$a(y) := \frac{1}{v\left(G^{-1}(x)\right)}, \quad b(y) := \frac{D\left(G^{-1}(x)\right)}{v\left(G^{-1}(x)\right)}.$$

The function $u_j^{1/2}(y)$ in (33) is an output of the first transport step in the operator splitting procedure (9) (see section 2).

Following a standard FVM strategy to approximate (31), one obtains

$$h_i F\left(u_i^j\right) - \int_{y_{i-1}}^{y_i} F(u(y, t_{j-1}))\, dy$$

$$- \tau a_i \left(b_i \frac{u_{i+1}^j - u_i^j}{\frac{h_{i+1}+h_i}{2}} - b_{i-1} \frac{u_i^j - u_{i-1}^j}{\frac{h_i+h_{i-1}}{2}} \right) = 0 \qquad (34)$$

for $i = 1, ..., M$, where $h_i = y_i - y_{i-1}$ and $a_i := a(y_i - h_i/2)$ and $b_i = b(y_i)$. Note that $u_i^j \approx u(y_i - h_i/2, t_j)$. Due to the boundary conditions, we complete $u_0^j = C^\circ(t_j)$ and $u_{M+1}^j = u_M^j$.

The resulting nonlinear algebraic system can be solved by a standard Newton iterative method using analytical linearisation. Another possibility is to use linearisation by a relaxation scheme that was developed in [13, 14] and has been justified in [1, 2, 11, 21], etc. (see [16] for more details).

The crucial point in the finite volume discretization method of (31) (that represents, in a discrete form, the mass balance property of the original analytical equation) is the evaluation of the integral in (34). We now show how to compute such integrals exactly.

The function $u(x, t_{j-1})$ in (34) is given by (33), so one has to compute

$$\int_{y_{i-1}}^{y_i} F(u_j^{1/2}(y))\, dy. \qquad (35)$$

The function $u_j^{1/2}$ consists of constants and rarefaction waves. The constant parts, although they do not fit to computational grids, make no difficulties in computations of (35). In the case of rarefaction waves (that are, in general, not available in an analytical form), an application of numerical quadrature for integral in (35) can lead to mass balance violations and solution errors.

To avoid such errors, we propose a procedure to evaluate the integral in (35) exactly by evaluating the rarefaction waves only in some finite number of discrete points.

Note that $w = F(u)$. Let us denote

$$J(\alpha, \beta; t_0) := \int_\alpha^\beta w^*(y, t_0)\, dy\,. \qquad (36)$$

The function w^* in (36) represents the rarefaction wave that starts at $t = 0$ as a constant function with not acceptable shock $y_0^{(na)}$ located at time $t = 0$ at the origin, i.e., $y_0^{(na)}(0) = 0$. The position of this shock at $t = t_0$ will be denoted by $\xi := y_0^{(na)}(t_0)$ and is given for isotherms (4)–(6) by

$$\xi = \begin{cases} 0 & p < 1 \text{ (Freundlich and the mixed type of isotherm),} \\ t_0 & p > 1 \text{ (Freundlich and the mixed type of isotherm),} \\ \frac{1}{1+a} t_0 & \text{Langmuir type of isotherm.} \end{cases}$$

We consider first the case $\xi < \alpha < \beta$, the case $\alpha < \beta < \xi$ (that occurs for Freundlich isotherms with $p > 1$) will be treated afterwards.

To evaluate $J(\alpha, \beta; t_0)$, one can first compute the values $J(\xi, \alpha; t_0)$ and $J(\xi, \beta; t_0)$ and then use

$$J(\alpha, \beta; t_0) = J(\xi, \beta; t_0) - J(\xi, \alpha; t_0)\,.$$

To compute $J(\xi, \beta; t_0)$, we track the acceptable shock $y_1^{(a)}(t_0) = \beta$ backward in time until $t = 0$, and we denote its initial (not yet known) position by $h := y_1^{(a)}(0)$. Clearly, a constant function $w(y, 0)$ that has the nonzero value $w(y, 0) \equiv A := w^*(\beta, t_0)$ only in interval $(0, h)$ will be transported to $w^*(y, t_0)$ at $t = t_0$ (see figure 7 for an illustration). As the variable w is mass conservative, one obtains $J(\xi, \beta; t_0) = Ah$.

To determine the value Ah, one can use the fact that the rarefaction wave meets the front shock at $t = t_0$, i.e.,

$$t_0 f'(A) = \beta, \qquad t_0 \frac{f(A)}{A} = \beta - h\,. \qquad (37)$$

From (37), one obtains that

$$\begin{aligned} Ah &= A(\beta - (\beta - h)) \\ &= t_0(Af'(A) - f(A)) \\ &= \beta \left(A - \tfrac{f(A)}{f'(A)} \right). \end{aligned}$$

Hence

$$J(\xi, \beta; t_0) = \beta \left(F(u^*(\beta, t_0)) - u^*(\beta, t_0) F'(u^*(\beta, t_0)) \right). \qquad (38)$$

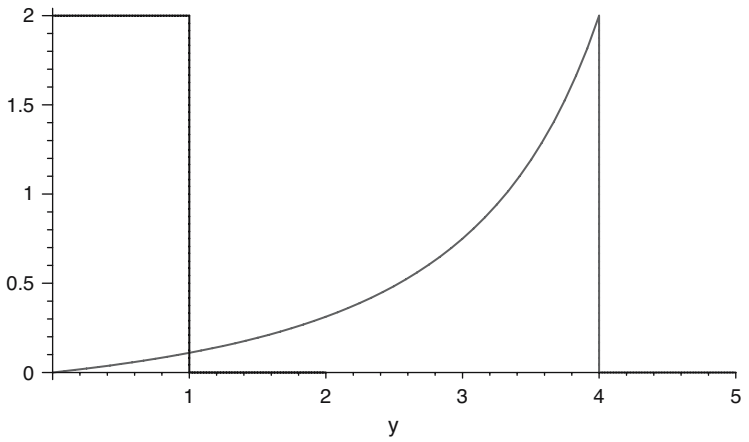

Figure 7 Constant function of value $A = 2$ at $t = 0$ with $h = 1$ that develops to rarefaction wave $w^*(\beta, t_0)$ at $t_0 = 6$ with $\xi = 0$ and $\beta = 4$ for the case of Freundlich isotherm with $p = 1/2$. Both areas are identical.

Finally, for the case that $\beta < \xi$, we have to evaluate $J(\beta, \xi; t_0)$ (see also the figure 8). One has, instead of (37),

$$t_0 f'(A) = \beta, \qquad t_0 \frac{f(A)}{A} = \beta + h\,, \tag{39}$$

and one obtains

$$Ah = A(\beta + h - \beta) = t_0(f(A) - Af'(A)) = \beta\left(\frac{f(A)}{f'(A)} - A\right).$$

As $J(\beta, \xi; t_0) = -J(\xi, \beta; t_0)$, (38) is also valid for this case.

Summarising, to compute the integral in (35) exactly, one needs to determine the values of rarefaction waves only for some finite set of points β and to apply (38).

If no analytical form of rarefaction wave is known, one can find the values $A = w^*(\beta, t_0) = F(u^*(\beta, t_0))$ by solving the equation $f'(A) = \beta/t_0$ with respect to A numerically (see also section 3.4).

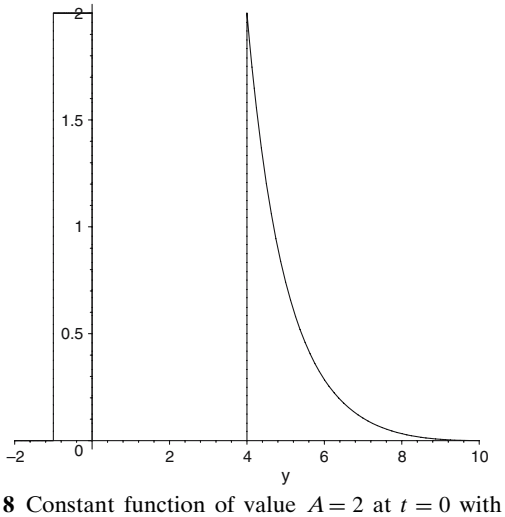

Figure 8 Constant function of value $A = 2$ at $t = 0$ with $h = 1$ that develops to rarefaction wave $w^*(\beta, t_0)$ at $t_0 = 10$ with $\beta = 4$ and $\xi = 10$ for the case of Freundlich isotherm with $p = 3/2$. Both areas are identical.

5. Numerical experiments

In this section we describe numerical experiments that confirm the applicability of the methods described above for transport problems with nonlinear sorption.

First, the exact solutions for the equation (if $d = 0$)

$$\partial_t F(u) + \partial_x u - d\,\partial_{xx} u = 0, \tag{40}$$

$$u(0, x) = 1,\ x \in (0, 1), \quad u(0, x) = 0,\ x \notin (0, 1),$$
$$u(t, 0) = 0,\ t > 0$$

for F given by (4) and (5) were implemented using the package Maple 7.0 [20] (see figures 1–8 in previous sections).

Such solutions can be directly constructed using definitions (17) if $t \in (0, t_1)$, where t_1 is a time when a rarefaction wave meets the shock in front. For the case when the speed of shock must be determined by solving ODE (24), built-in Maple procedures can be used to obtain very precise numerical solutions.

Finally, to solve the general form of (40) with $d \neq 0$ numerically, the operator splitting method was implemented as described in section 2. The transport part was solved in section 3 and the discretisation of diffusive part with an analytical linearisation used in Newton's method in section 4.

Extensive tests were done for the most interesting (and the most complicated case) of Freundlich isotherm with $p < 1$. As $F'(0) = \infty$, a modification of the analytical linearisation used in Newton's method must be done.

We avoided a modification (a "regularisation") of the function F itself. To modify $F'(u)$ only, a small

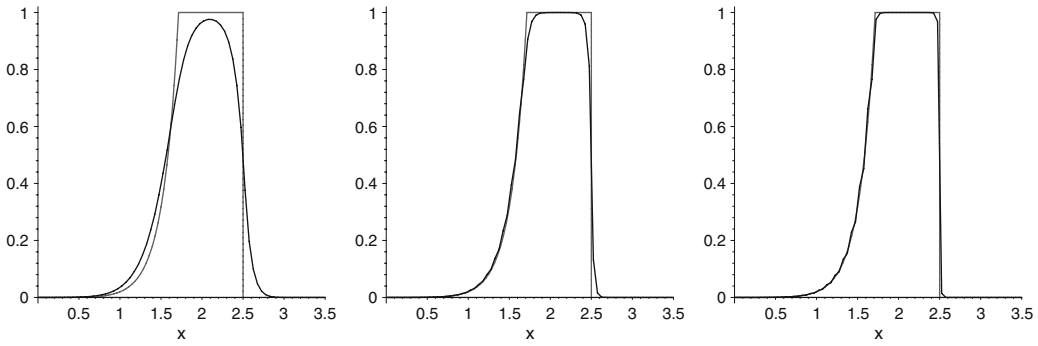

Figure 9 Numerical solutions of $\partial_t \left(u + u^{3/4}\right) + \partial_x u - d\partial_{xx} u = 0$ for $d = 10^{-2}, 10^{-3}, 10^{-4}$ at $t = 3$ (from left to right) that are compared with the exact solution for $d = 0$.

parameter ϵ (to be set by the user) was chosen and $F'(u)$ was replaced by $\tilde{F}'(u)$, where

$$\tilde{F}'(u) := \begin{cases} F'(u)\,, & \text{if } u \geq \epsilon \\ F'(\epsilon)\,, & \text{if } u < \epsilon\,. \end{cases} \tag{41}$$

The implementation of iterative procedure for Newton method was realised using C-language procedures of *Numerical Recipes* [25].

To illustrate that the method described in this paper can be applied for $d \approx 0$ in (40), the following examples were realised. The grid step in all examples was chosen to be uniform $h_i \equiv h = 0.05$.

Firstly, system (40)–(41) was computed for a smaller time ($t = 3$) before the rarefaction wave meets the shock in front. These computation were realised for $d = 10^{-2}$, 10^{-3} and 10^{-4}, see figure 9, where the numerical solution is compared with the exact solution for $d = 0$ to judge the influence of nonzero physical diffusion. All computations were realised using only two time steps, i.e., $\tau = 1.5$, and the Courant number was approximately 17. Clearly, the method produces for different d different results, which is not the case for many numerical methods when solving (40) with very small diffusion.

Secondly, analogous tests were carried out for larger times with rarefaction wave behind the shock in front. Again (figure 10), the method can produce clearly different results for different small diffusion coefficients. In all computations, $\tau = 1.5$ with the Courant numbers varying around the value 17.

6. Conclusions

In this paper semi-analytical solutions for one-dimensional problems of contaminant transport with nonlinear adsorption were constructed. The method is based on operator splitting where the convective transport is solved exactly for a piecewise constant initial condition, and the diffusive transport is solved by a finite volume method. For small diffusion coefficients, the advantage of this method is that very large time steps can be used to obtain precise numerical results.

Such semi-analytical solutions can be utilised as benchmark examples for numerical packages. Moreover, the solution procedure presented here can be used for inverse problems that deal with the determination of soil properties.

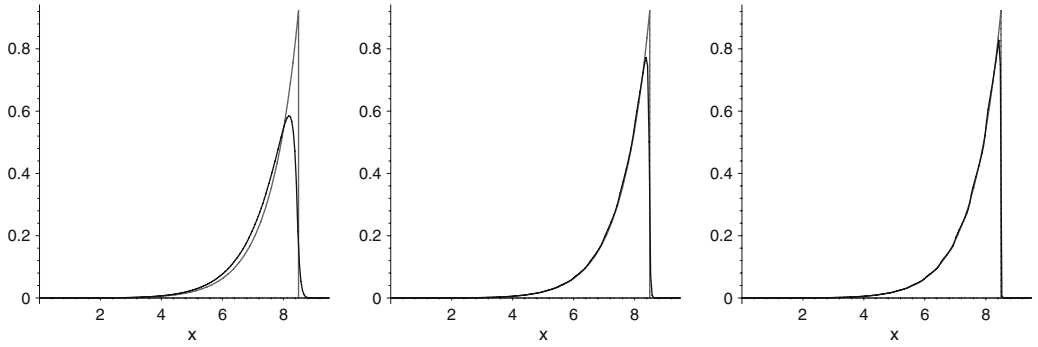

Figure 10 Numerical solutions of $\partial_t (u + u^{3/4}) + \partial_x u - d\partial_{xx} u = 0$ for $d = 10^{-2}, 10^{-3}, 10^{-4}$ at $t = 15$ (from left to right) that are compared with the exact solution for $d = 0$.

Acknowledgments This work was funded by the Federal Ministry of Economics and Technology (BMWi) under the contract number 02 E 9148 2 and the second author was also partially supported by grants MSM 262100001 and GARC 201/03/0570.

References

1. Babušikova, J.: Application of relaxation scheme to degenerate variational inequalities. Appl. Math. **46**, 419–439 (2001)
2. Bänsch, E.: Numerical experiments with adaptivity for the porous medium equation. Acta Math. Univ. Comen. (N.S.) **64**, 425–454 (1995)
3. Barrett, J., Kappmeier, H., Knabner P.: Lagrange-Galerkin approximation for advection-dominated nonlinear contaminant transport in porous media. In: Computational Methods in Water Resources X, vol. 1, pp. 299–307. (1994)
4. Barrett, J., Kappmeier, H., Knabner, P.: Lagrange-Galerkin approximation for advection-dominated contaminant transport with nonlinear equilibrium or non-equilibrium adsorption. In: Helmig, R., et al. (ed.) Modelling and Computations in Environmental Science, pp. 36–48. Vieweg, Braunschweig (1997)
5. Dafermos, C.: Polygonal approximation of solutions of the initial value problem for a conservation law. J. Math. Anal. Appl. **38**, 33–41 (1972)
6. Dawson, C.: Analysis of an upwind – mixed finite element method for nonlinear contaminant transport equations. SIAM J. Numer. Anal. **35**(5), 1709–1729 (1998)
7. Dawson, C., Van Duijn, C., Grundy, R.: Large time asymptotics in contaminant transport in porous media. SIAM J. Appl. Math. **56**, 965–993 (1996)
8. Dawson, C., Van Duijn, C., Wheeler, M.: Characteristic-Galerkin methods for contaminant transport with non-equilibrium adsorption kinetics. SIAM J. Numer. Anal. **31**(4), 982–999 (1994)
9. Frolkovič, P., Geiser, J.: Numerical simulations of radionuclides transport in double porosity media with sorption. In: Handlovicova, A., et al. (ed.) Algoritmy 2000, pp. 28–36. Slovak University of Technology, Bratislava (2000)
10. Grundy, R., Van Duijn, C., Dawson, C.: Asymptotic profiles with finite mass in one-dimensional contaminant transport through porous media. Q. J. Mech. Appl. Math. **1**(47), 69–106 (1994)
11. Handlovičova, A.: Solution of Stefan problems by fully discrete linear schemes. Acta Math. Univ. Comen., N.S. **67**(2), 351–372 (1998)
12. Holden, H., Karlsen, K., Lie, K.-A.: Operator splitting methods for degenerate convection–diffusion equations: II. Numerical examples with emphasis on reservoir simulation and sedimentation. Comput. Geosci. **4**, 287–323 (2000)
13. Jäger, W., Kačur, J.: Solution of doubly nonlinear and degenerate parabolic problems by relaxation schemes. Math. Model. Numer. Anal. **29**, 605–627 (1995)
14. Kačur, J.: Solution to strongly nonlinear parabolic problems by a linear approximation scheme. IMA J. Num. Anal. **19**, 119–154 (1999)
15. Kačur, J., van Keer, R.: Solution of contaminant transport with adsorption in porous media by the method of characteristics. M2AN **35**(5), 981–1006 (2001)
16. Kačur, J., Frolkovič, P.: Semi-analytical solutions for contaminant transport with nonlinear sorption in 1D. Preprint 24, Interdisziplinäres Zentrum für Wissenschaftliches Rechnen, Heidelberg (2002)
17. Kružkov, S.: First order quasi-linear equations in several independent variables. Math. USSR Sbornik **10**(2), 217–243 (1970)
18. LeVeque, R.J.: Numerical methods for conservation laws, Lectures in Mathematics. ETH Zürich, Birkhäuser-Verlag, Basel (1992)
19. LeVeque, R.J.: Finite Volume Methods for Hyperbolic Problems, Cambridge Texts in Applied Mathematics. Cambridge University Press (2002)
20. Maple 9.5, http://www.maplesoft.com
21. Mikula, K.: Numerical solution of nonlinear diffusion with finite extinction phenomena. Acta Math. Univ. Comen., N.S. **2**, 223–292 (1995)
22. Ohlberger, M.: Higher order finite volume methods on self-adaptive grids for convection dominated reactive transport problems in porous media. Comput. Vis. Sci. **7**(1), 41–51 (2004)
23. Olejnik, O.: Discontinuous solutions of non-linear differential equations. Am. Math. Soc. Transl. **2**(26), 95–172 (1963)
24. Olejnik, O.: Uniqueness and stability of the generalized solution of the Cauchy problem for a quasi-linear equation. Am. Math. Soc. Transl. **2**(33), 285–290 (1963)
25. Press, W.H., Teukolsky, S.A., Vetterling, W.T., Flannery, B.P.: Numerical Recipes in C. The Art of Scientific Computing. Cambridge University Press (1992)
26. Sheng, D., Smith, D.W.: Analytical solutions to the advective contaminant transport equation with nonlinear sorption. Int. J. Numer. Anal. Methods Geomech. **23**, 853–879 (1999)
27. Van Duijn, C., Knabner, P.: Solute transport in porous media with equilibrium and nonequilibrium multiple site adsorption: Traveling waves. J. Reine Angew. Math. **415**, 1–49 (1991)